Supplement of Atmos. Chem. Phys., 26, 4685–4709, 2026
https://doi.org/10.5194/acp-26-4685-2026-supplement

Atmospheric Chemistry and Physics
Open Access
EGU

Supplement of

Natural and anthropogenic influence on tropospheric ozone variability over the Tropical Atlantic unveiled by satellite, reanalyses and in situ observations

Sachiko Okamoto et al.

Correspondence to: Sachiko Okamoto (okamoto.sachiko@nies.go.jp) and Juan Cuesta (cuesta@lisa.ipsl.fr)

S1 Altitude range of IAGOS data over the Atlantic

IAGOS has been providing a dense database of in situ observations of atmospheric compositions including ozone and CO by using commercial aircraft since 1994 (e.g., Petzold et al., 2015). Most of data are acquired in the extratropical upper troposphere/lower stratosphere (UTLS) and in the tropical upper troposphere when the aircraft attain cruise altitude between 9 and 13 km. The remaining data are collected during landing and take-off over more than 300 airports around the world. All IAGOS data during the two periods 13–15 February 2017 (ATom-2) and 17–20 October 2017 (ATom-3) were obtained over 10 km of altitude over the Atlantic in the Northern Hemisphere (Fig. S1).

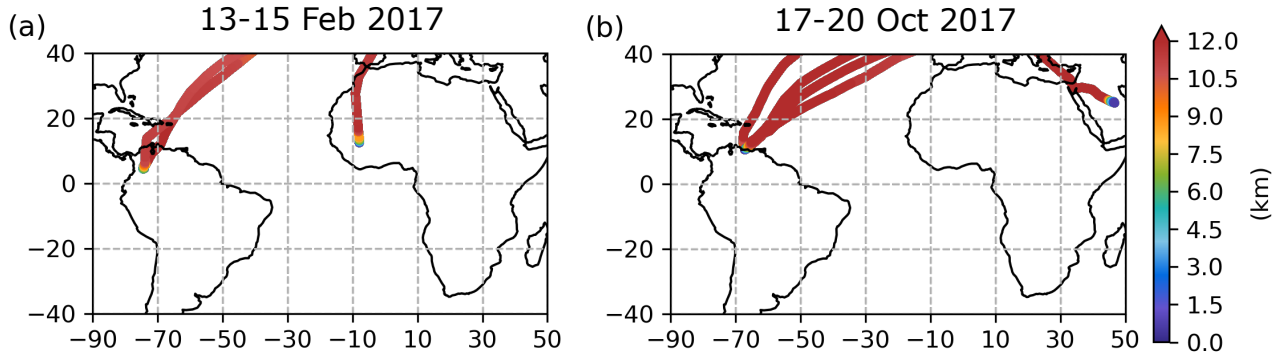

Figure S1: Flight tracks of IAGOS flights during (a) ATom-2 (13–15 February 2017) and (b) ATom-3 (17–20 October 2017).

S2 Source identification of ozone

We quantify the influence of biomass burning and urban emissions on the tropospheric ozone during ATom-2 and 3 according to the method of Bourgeois et al. (2021). The authors analyse in situ measurements of ozone (O_3) and H_2O, for defining air parcels with $O_3/H_2O > 1$ ppbv ppmv^{-1} and with $O_3/H_2O < 0.003$ ppbv ppmv^{-1} as strongly influenced by stratospheric air and by marine air, respectively. To quantify the respective influence of biomass burning and urban emissions on each air parcel, they use a pair of HCN (biomass burning tracer) and C_2Cl_4 (urban tracer). These two tracers are chosen because their lifetime is similar to that of CO (being between three and five months for these three tracers), and they have been used as a tracer in the previous studies. First, all sampled air masses are classified into four categories. For the region (40° S–40° N), air parcels are either defined as urban air (urban tracer > regional median, biomass burning tracer < regional median), biomass burning

air (biomass burning tracer > regional median, urban tracer < regional median), mixed pollution air (both urban and biomass burning tracers > regional median), and well-mixed and aged air (both urban and biomass burning tracers < regional median) corresponding to rather clean or background conditions. The normalized excess mixing ratio (NEMR) of biomass burning and urban tracers is calculated according to Eq. (1):

$$NEMR_X = \Delta X/\Delta CO, \quad (1)$$

where $NEMR_X$ is the normalized excess mixing ratio of compound X (i.e., X = HCN or C_2Cl_4) to CO, and ΔX (ΔCO) is the difference between the mixing ratio of compound X (CO) and its background level. The background levels are defined as the average mixing ratio in well-mixed and aged air masses. The respective influence of urban and biomass burning emissions (F_X) is then calculated as the ratio of the NEMR of compound X to the average emission ratio of compound X (ER_X) as follows:

$$F_X = NEMR_X/ER_X, \quad (2)$$

Bourgeois et al. (2021) use 5.7 pptv ppbv^{-1} (HCN/CO) and 0.03 pptv ppbv^{-1} (C_2Cl_4/CO) as ERs of biomass burning and urban air according to Andreae (2019) and Kondo et al. (2004).

S3 Lightning

Scientific observations of lightning occurrence have been recorded from the space and the ground. The Lightning Imaging Sensor – Optical Transient Detector (LIS/OTD) dataset by two lightning detection sensors: the OTD on the Orbview-1 satellite and the LIS aboard the Tropical Rainfall Measuring Mission (TRMM) satellite have been most widely used. However, the LIS/OTD 0.5 Degree High Resolution Monthly Climatology (HRMC) covers the period 1995–2014, and is not updated (Cecil et al., 2014). The World Wide Lightning Location Network (WWLLN) is a global network monitoring lightning activity by very low frequency radio sensors (Dowden et al., 2002). Recently, a global, high-resolution gridded time series and climatology of lightning stroke density, the WWLLN Global Lightning Climatology (WGLC) has been published (Kaplan and Lau, 2021a) and is freely available at 0.5° and 5 arcmin spatial resolution and with daily and monthly temporal resolution (Kaplan and Lau, 2021b, last access: 19 April 2023). Kaplan and Lau (2021a) compared climatological mean annual lightning density between the WGLC and the LIS/OTD, even though the periods of the record are not overlapping and the lightning phenomenon observed, i.e., strokes in the WGLC and flashes in the LIS/OTD, is different. The LIS/OTD captured more lightning than the WGLC, particularly over land. The area of the greatest difference was in the eastern Congo Basin which was also a hotspot for lightning in the WGLC. Other regions where the WGLC had lower lightning than the LIS/OTD were in the Western High Plateau of Cameroon and northwestern South America. In the Northern Hemisphere and over the oceans, the differences were smaller.

S4 Monthly evolution of lightning and fire activities

The climate in the tropics is characterised by alternating wet and dry seasons depending on the position of the ITCZ. It moves north in the Northern Hemisphere summer and south in the Northern Hemisphere winter. According to the maps presented in Fig. S2–S3, lightning and fire activities can be observed throughout the year in both, the African and the South American continents, with large seasonal variability, clearly associated with the ITCZ annual shift. Estimations of the regional lightning source altitudes by the satellite (derived by Peterson 2022) suggest that the source altitude distributions peak at 10–11 km altitude over the Amazon and the Congo Basins. In the La Plata Basin and South Africa, they peak at lower altitude. Therefore, wind vectors at 10 km of altitude have been added in Fig. S2 and 2a–b. In February, the highest lightning densities are observed in the Gulf of Guinea, Central and Southern Africa, and over South America (Fig. S2a). This clearly shows that this is the location where strong ascending motions within the troposphere are expected, which may bring air pollutants emitted from the surface such as ozone precursors up to the middle and upper troposphere. In May, convective activity shifts northwards in location as suggested by the decrease of lightning in South America and peaks over Colombia and Venezuela (Fig. S2b) and an increase over the African Sahel in a vast west-to-east band. While lightning density distribution in August is quite similar to the previous month, the density decreases in Western Africa (Fig. S2c). In this period (May–August), deep convection likely affects atmospheric circulation mainly north of the equator. In November, the centre of lightning activities moves southwards as a consequence of the ITCZ shift (Fig. S2d). The highest lightning densities are detected in the Congo Basin, Brazil, Northern and Western South America.

According to FRP maps presented in Fig. S3, fire activity also varies with the ITCZ annual shift. In February, enhancement of FRP can be observed in the Caribbean North, Southern Cone, Western and Central Africa (Fig. S3a). Following the wind flow (shown at 3 km of altitude in Fig. S3), trace gases and smoke emitted by biomass fires are then expected to largely affect the Tropical Atlantic. In May, while the location of the highest FRP values is similar to previous months, the intensity decreases in South America and the Sahel south of the Sahara Desert, and increases in the Congo Basin (Fig. S3b). In August, the fire intensity is the highest over the Congo Basin and Brazil (Fig. S3c). In November, fires are still detected in South America and Southern Africa, and restarts over the Sahel south of the Sahara Desert (Fig. S3d).

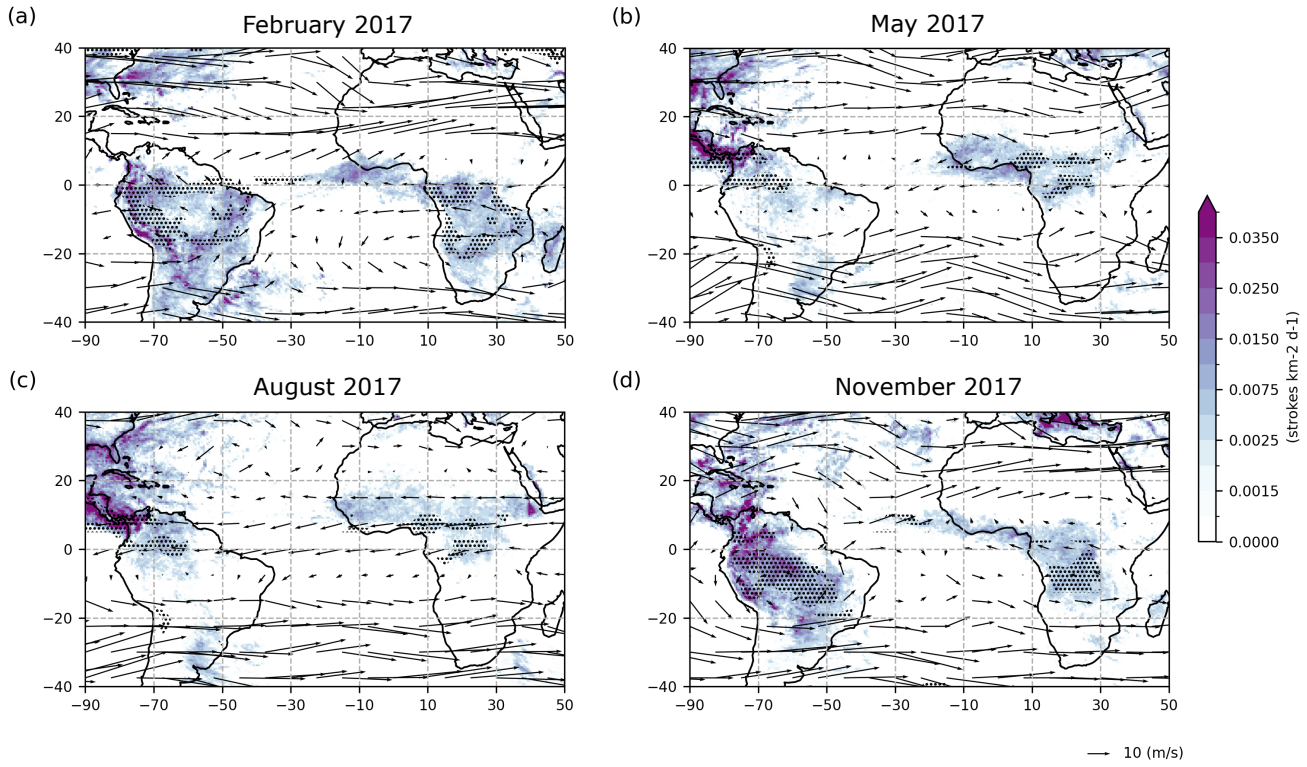

Figure S2: Monthly WGLC lightning density in (a) February, (b) May, (c) August and (d) November 2017. Winds at 10 km of altitude from ERA5 are indicated by black arrows. Black dots indicate areas with OLR < 220 W m^{-2}.

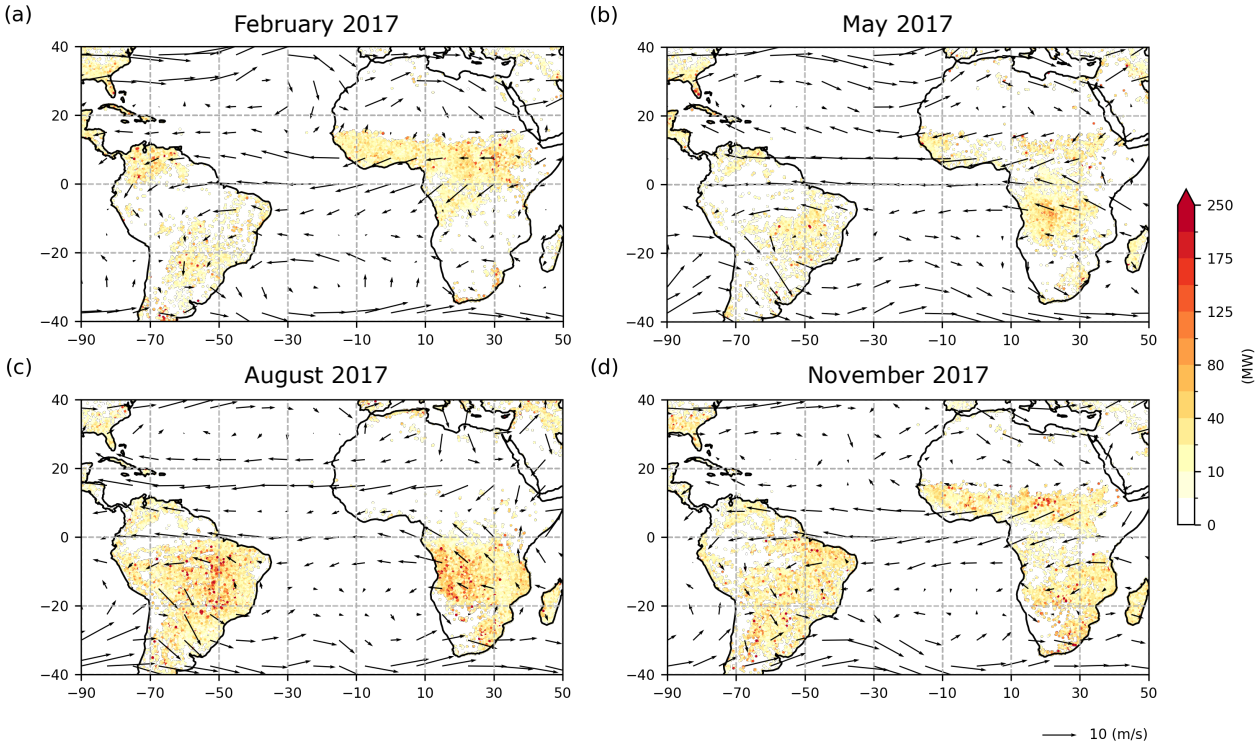

Figure S3: Monthly fire radiative power (FRP) of presumed vegetation fire in (a) February, (b) May, (c) August and (d) November 2017. Winds at 3 km altitude from ERA5 are indicated by black arrows.

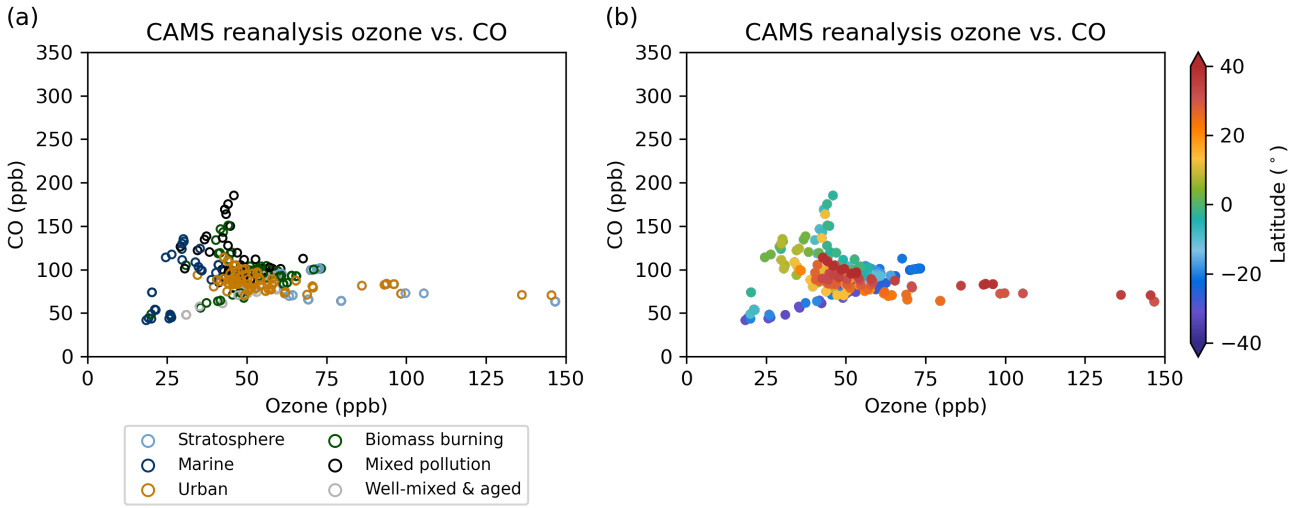

85

Figure S4: Scatter plots of CO vs. ozone for air masses sampled by ATom-2 derived from CAMS reanalysis. Colours indicate (a) the air masses classification into six categories (idem as Figs. 9a and 10a) and (b) the latitude location.

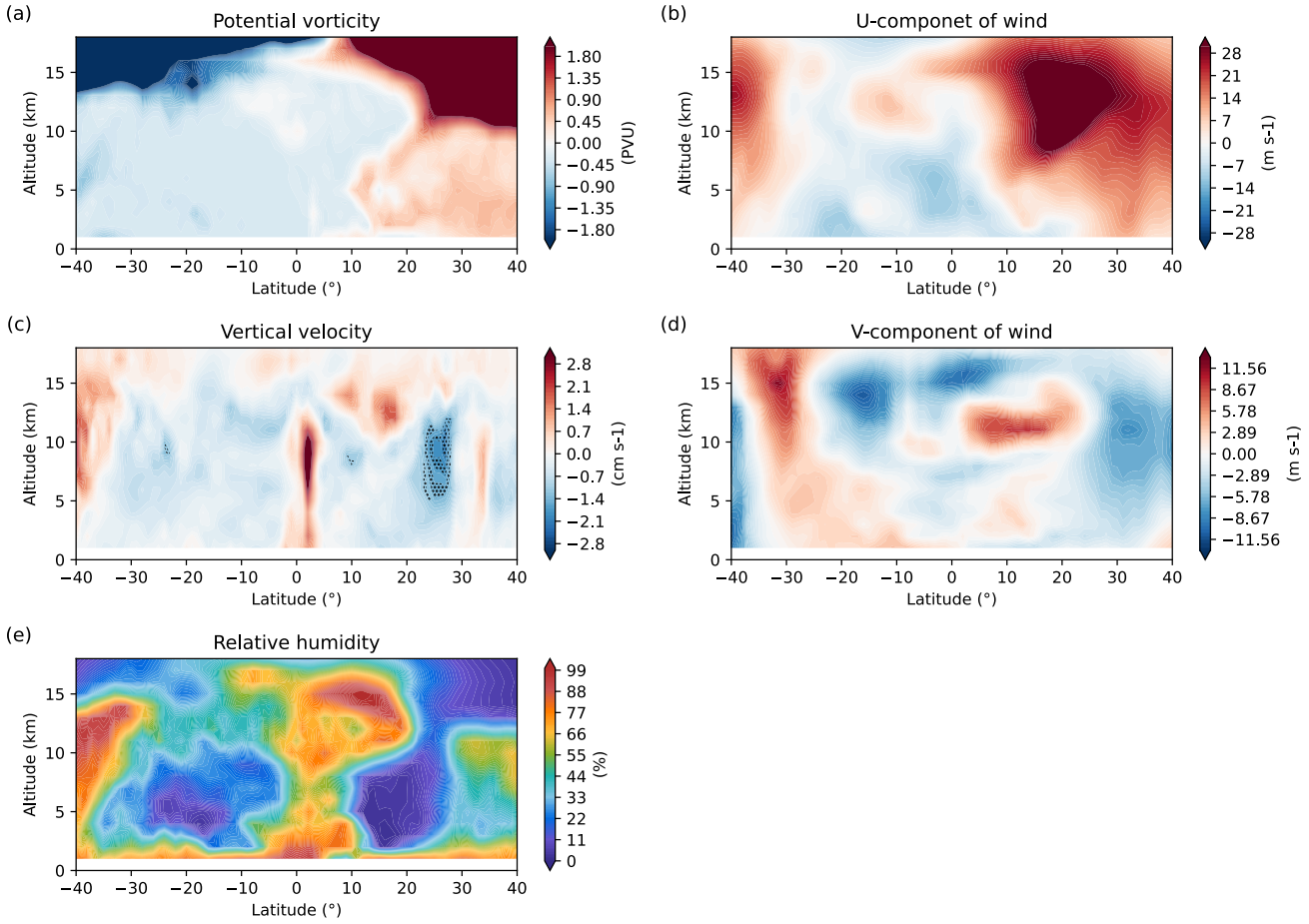

90 **Figure S5: Vertical profiles of meteorological factors from ERA5 for the period from 13 to 15 February 2017. (a) Potential vorticity, (b) u wind component, (c) vertical velocity, (d) v wind component, and (e) relative humidity averaged for the period from 13 to 15 February 2017, and extracted along the flight track. Positive u and v wind components is from the west and the south, respectively.**

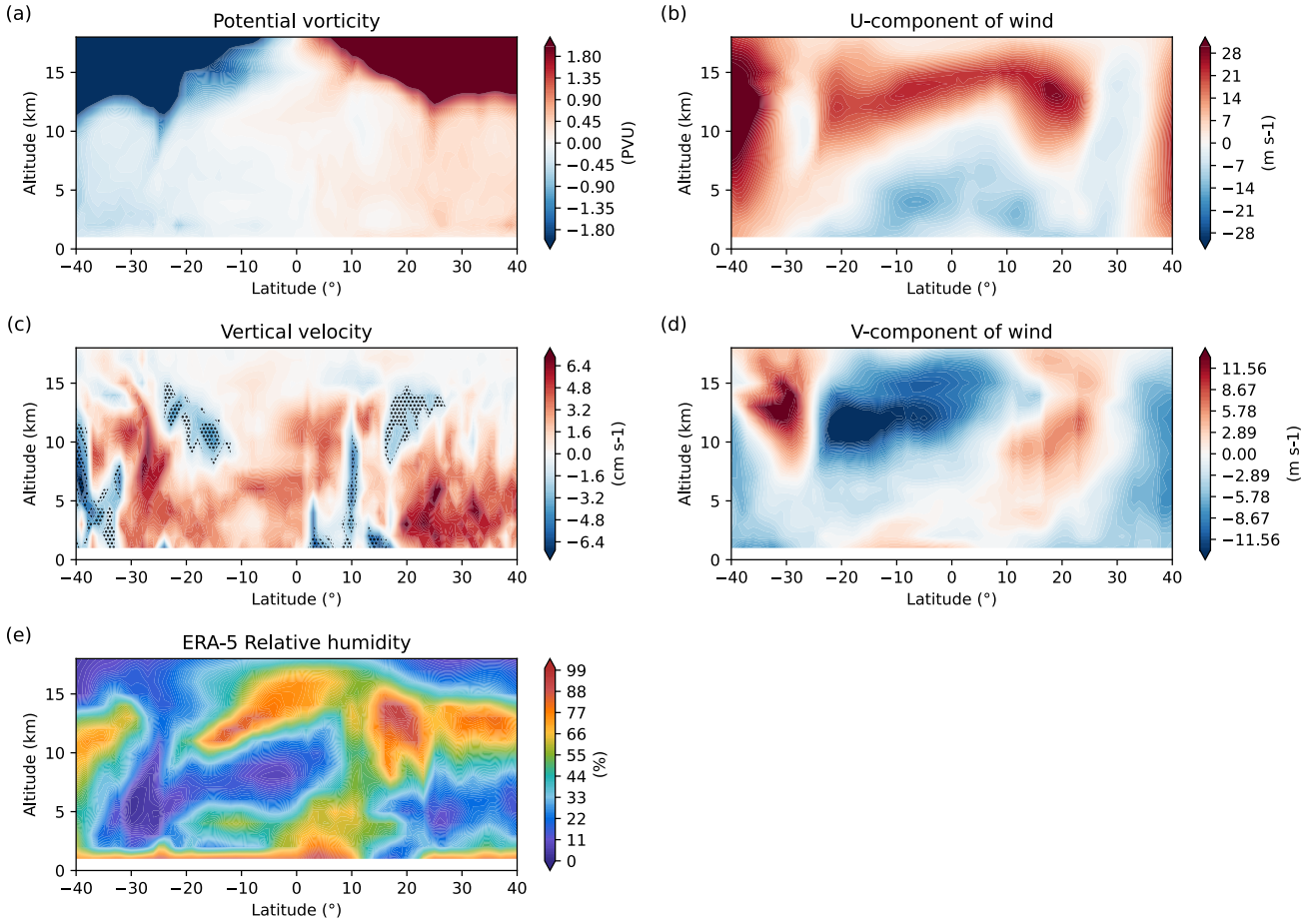

Figure S6: Vertical profiles of meteorological factors from ERA5 for the period from 17 to 20 October 2017. (a) Potential vorticity, (b) u wind component, (c) vertical velocity, (d) v wind component, and (e) relative humidity averaged for the period from 17 to 20 October 2017, and extracted along the flight track. Positive u and v wind components is from the west and the south, respectively.

References

Cecil, D. J., Buechler, D. E. and Blakeslee, R. J.: Gridded lightning climatology from TRMM-LIS and OTD: Dataset description, Atmos. Sci., 135, 404–414, https://doi.org/10.1016/j.atmosres.2012.06.028, 2014.

Dowden, R. L., Brundell, J. B. and Rodger, C. J.: VHF lightning location by time of group arrival (TOGA) at multiple site, J. Atmos. Sol.-Terr. Phys., 64, 817–830, https://doi.org/10.1016/S1364-6826(02)00085-8, 2002.

Kaplan, J. O. and Lau, K. H.-K.: The WGLC global gridded lightning climatology and time series, Earth Syst. Sci. Data, 13, 3219–3237, https://doi.org/10.5194/essd-13-3219-2021, 2021a.

Kaplan, J. O. and Lau, K. H.-K.: The WWLLN Global Lightning Climatology and timeseries (WGLC) (v2022.0.0), Zenodo [data set], https://doi.org/10.5281/zenodo.6007052, 2021b.

Peterson, M.: FORTE Measurements of Global Lightning Altitudes, Earth Sp. Sci., 9, 1–22, https://doi.org/10.1029/2022EA002404, 2022.

Petzold, A., Thouret, V., Gerbig, C., Zahn, A., Brenninkmeijer, C. A. M., Gallagher, M., Hermann, M., Pontaud, M., Ziereis, H., Boulanger, D., Marshall, J., Nédélec, P., Smit, H. G. J., Friess, U., Flaud, J.-M., Wahner, A., Cammas, J.-P., Volz-Thomas, A., and IAGOS TEAM: Global-scale atmosphere monitoring by in-service aircraft – current achievements and future prospects of the European Research Infrastructure IAGOS, Tellus B, 6, 1–24, https://doi.org/10.3402/tellusb.v67.28452, 2015.